Turkish Journal of Physics

http://journals.tubitak.gov.tr/physics/

Research Article

Turk J Phys
(2014) 38: 104 – 110

doi:10.3906/fiz-1301-1

Properties of PbS thin films grown on glass and layered GaSe crystal substrates by chemical bath deposition

Mevlüt KARABULUT[1,*], Hüseyin ERTAP[1], Hasan MAMMADOV[1], Güventürk UĞURLU[1], Mustafa Kemal ÖZTÜRK[2]

[1]Department of Physics, Faculty of Arts and Sciences, Kafkas University, Kars, Turkey
[2]Department of Physics, Faculty of Science, Gazi University, Ankara, Turkey

Received: 04.01.2013 • **Accepted:** 13.09.2013 • **Published Online:** 17.01.2014 • **Printed:** 14.02.2014

Abstract: PbS thin films were grown on glass and GaSe crystal substrates by chemical bath deposition and their structural, morphological, optical, and electrical properties were investigated. PbS films grew in cubic structure with lattice constants equal to 5.9315 Å and 5.9362 Å for films grown on glass and GaSe crystal, respectively. The band gaps of the PbS films were determined to be 1.60 eV. The long wavelength tails of absorption spectra showed exponential dependence on the incident photon energy according to the Urbach–Martiensen model. Electrical properties of PbS films were investigated by the van der Pauw method, which showed that PbS films were p and n type depending on the temperature. At low temperatures, the p-type conductivities of PbS thin films grown on glass and GaSe substrates were found to be due to the ionization of acceptor centers with energies of 94.50 meV and 36.50 meV, respectively, while at higher temperatures the n-type conductivities were found to be determined by the ionization of donor centers with energies of 226.50 meV and 310 meV, respectively. The sheet charge carrier concentration and mobility of PbS film grown on GaSe substrate were, in general, higher than those of films grown on glass substrate.

Key words: PbS thin films, chemical bath deposition, optical properties, electrical properties

1. Introduction

Lead sulfide (PbS) bulk crystal with a direct narrow band gap of 0.41 eV has been widely used in near-IR detectors [1]. PbS thin films have applications in different fields such as IR detectors [1], display devices [2], Pb^{+2} ion-selective sensors [3], and solar control coatings [4]. PbS thin films are also utilized in LEDs [5], humidity and temperature sensors [6,7], and in optical switching [8] due to their third-order nonlinear optical properties [9]. These properties are related to the growth conditions and characteristics of substrates. Among several growth techniques such as electrodeposition, spray pyrolysis, and microwave heating, the chemical bath deposition (CBD) technique is useful to grow PbS films at low temperatures [10–13]. CBD is relatively simple, inexpensive, and appropriate for large area coating. Furthermore, good quality films can be grown by this technique.

The characteristics of PbS thin films synthesized by CBD show strong dependence on the growth conditions and methods [10–21]. PbS films grown by CBD have been found to consist of particles of different sizes and hence of different band gaps [10]. The sizes of nanoparticles can be changed by varying the pH and growth temperature in CBD, making this technique valuable in nanotechnology [10]. It was found that the

*Correspondence: mevlut@kafkas.edu.tr

optical band gap decreases with increasing pH and temperature of the chemical bath, while its values increase with decreasing particle size [10]. The PbS particles deposited by CBD at room temperature using lead acetate and thiourea were found to be 20 nm in size [14]. The structural and surface morphological investigation of PbS films grown by hydrothermal method showed that the films consisted of crystalline nanoparticles of different sizes and shapes [15–17]. Another method used to grow PbS films is the successive ionic layer adsorption and reaction (SILAR) technique [18–21].

Because of the relatively large Bohr exciton radius, the band gap of PbS thin films can be tailored over a wide range by reducing the particle size. This makes the quantum confinement effect important in these films [22–26].

It would be interesting to see the substrate effect on the properties of PbS thin films since the main focus has been on PbS films grown on glass substrates. For example, growth of PbS thin films on layered GaSe crystals is expected to cause low density of states at the interface [27]. Different from nonlayered structures, the Se atoms have no dangling bonds at the (0001) surface of layered GaSe crystals. The interlayer bonding in these crystals is van der Waals. Hence, PbS films grown on GaSe layers and the Se atoms at the surface are expected to bond via van der Waals interaction. The lattice parameters in these kinds of van der Waals heterojunctions may allow the formation of different junctions depending on the compatibility of the bonding natures in lattices [28–30]. In the present work, PbS films were grown on GaSe crystal substrate by CBD, and the structural, morphological, optical, and electrical properties of the films were investigated. PbS films were also grown on glass substrates under the same conditions and their properties were studied for comparison.

2. Experimental details

PbS thin films were deposited onto glass substrate and GaSe crystal substrate by CBD. GaSe substrate was prepared by cleaving layers from the GaSe crystals grown by Bridgman's method [31,32] with a razor blade. The thicknesses of the 1 cm $\times$ 3 cm substrates were in the 100–500 μm range. No chemical process was applied to these naturally mirror-faced GaSe crystals prior to the growth process. On the other hand, glass substrates were chemically cleaned prior to the growth process. The chemical baths were prepared with 5 mL of 0.5 M lead acetate ($Pb(CH_3COO)_2.3H_2O$) and 6 mL of 1 M thiourea ($(NH_2)_2CS$). Sodium hydroxide (NaOH: 5 mL, 2 M) and triethanolamine ($N(CH_2CH_2OH)_3$: 2 mL, 1 M) were used to adjust the pH of the solution and as the complexing agent, respectively. The chemically cleaned glass substrate and GaSe substrate were immersed vertically into chemical solutions. Immersing processes were carried out for 120 min at 27 °C.

The structure of the films grown on both substrates was analyzed by X-ray diffraction (XRD) using Cu K_α radiation (λ = 1.5405 Å). The surface morphologies of the films were probed using a JEOL 440 model scanning electron microscope (SEM). Elemental analysis was carried out by energy dispersive analysis of X-rays (EDAX). The optical absorbance spectra were recorded using a PG Instruments T60 UV/VIS spectrophotometer. The electrical properties of the films were measured by the van der Pauw method using a Lakeshore Hall effect measurement system (HMS). Ohmic behavior of the contacts was confirmed by the current-voltage characteristics.

3. Results and discussion

The SEM image and EDAX analysis of the PbS film grown on glass substrate are given in Figure 1. EDAX analysis revealed that the Pb:S atomic ratio is close to one, while the SEM image shows that the surface of the films is like dendrites.

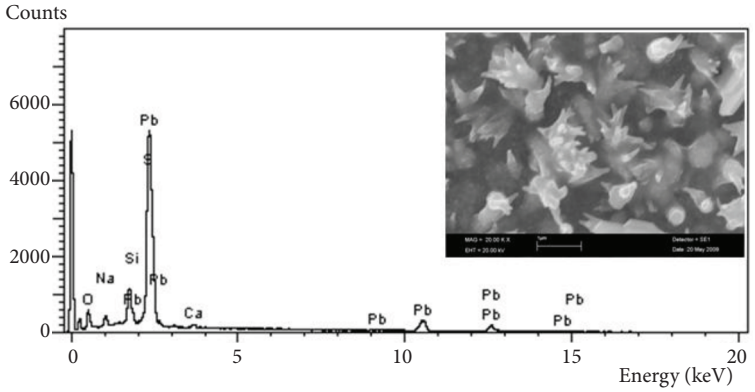

Figure 1. EDAX spectra and SEM image of PbS film grown on glass substrate.

The XRD spectra of PbS films grown on glass and GaSe substrates at room temperature are given in Figures 2a and b. The XRD spectrum of bulk GaSe crystal is also included in Figure 2b for comparison. The analysis showed that the PbS films grown on both glass and GaSe crystal substrates have fcc structures with lattice constants, a, equal to 5.9315 Å and 5.9362 Å, respectively, and belonging to the Fm-3m space group. The crystallite sizes of PbS thin films were determined using the Scherrer equation:

$$L = \frac{k\lambda}{B\cos\theta},$$

where L is the crystallite size; k is the shape factor taken as 0.9; λ is the X-ray wavelength used (0.15418 nm); B is the full width at half maximum (FWHM) of the diffraction peaks corresponding to (111), (200), (220), and (311) crystal planes, and θ is the diffraction angle of the line under consideration [14,33]. The crystallite size of PbS film grown on glass substrate was determined to be 20–100 nm, while the crystallite size of PbS film grown on GaSe substrate was shown to be much larger, 136–919 nm. A similar result was observed in our previous study of CBD grown MnS films [34].

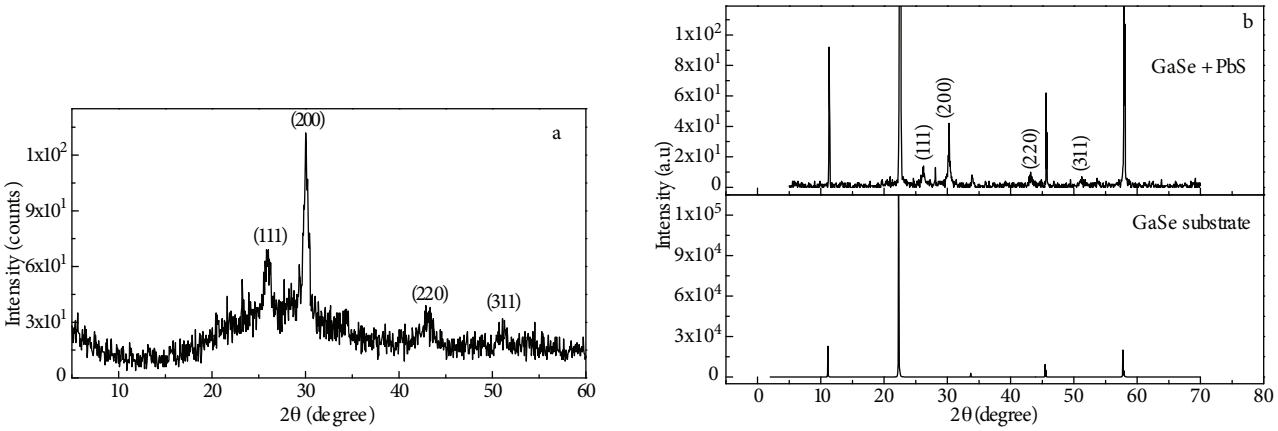

Figure 2. The XRD spectra of PbS films grown on **a)** glass substrate, **b)** GaSe crystal substrate.

The crystal structure of PbS films grown by CBD seems to be independent of the substrates used. PbS films grown on both glass and GaSe substrates were found to have a fcc structure that is the same as the bulk PbS structure. At the beginning of this study, it was expected that the PbS films deposited on layered GaSe

crystal would form a van der Waals heterojunction by repeating one of the polytypes of GaSe. There are 4 polytypes of GaSe and the lattice parameters of these polytypes are presented in the Table [35]. Clearly the lattice parameters and the space group of the PbS film grown on GaSe substrate are different from the lattice parameters of any of the polytypes of GaSe crystal. The reason for this may be the formation of a prelayer of sulfur atoms on which cubic PbS grows as in GaAs [36]. The Pb–S bond in PbS and the Se–Ga–Ga–Se bond in GaSe are much stronger than the van der Waals bond between layers; thus PbS thin films grow with a cubic structure rather than a hexagonal structure. Hence, only the quasi van der Waals junction (QvdWJ) can form at the PbS–GaSe intersection. A similar result was obtained for MnS films grown on GaSe [34].

Table. The lattice parameters of different polytypes of GaSe [35].

Polytype	a (Å)	c (Å)
$\varepsilon-$GaSe	3.755	15.95
$\beta-$GaSe	2.75	15.94
$\gamma-$GaSe	3.74	23.86
$\delta-$GaSe	3.75	31.989

The optical absorption spectra of PbS thin films grown on glass and GaSe substrates are shown in Figure 3. Absorption varies with incident photon energy as $(\alpha h\upsilon)^2 \sim (h\upsilon)$, indicating that PbS films have a direct optical band gap. Band gap energies were obtained by the extrapolation of the linear regions on the energy axis of the absorption curves to intercept the energy axis. The calculated band gap energies of PbS films grown on glass and GaSe substrates are found to be of 1.60 eV and 1.59 eV, respectively. The analysis of the long wavelength tail of the absorption spectra at 1.2 eV indicates that the tail varies exponentially with photon energy according to the Urbach–Martiensen model, $\alpha = \alpha_0 \exp[(h\nu - E_0)/E_U]$, where E_U is the Urbach energy. The Urbach energies calculated from the fits for PbS films grown on glass and GaSe substrates were found to be approximately 1.06 eV. These higher values of Urbach energies are indicative of lattice defects and disorders in PbS films [37,38].

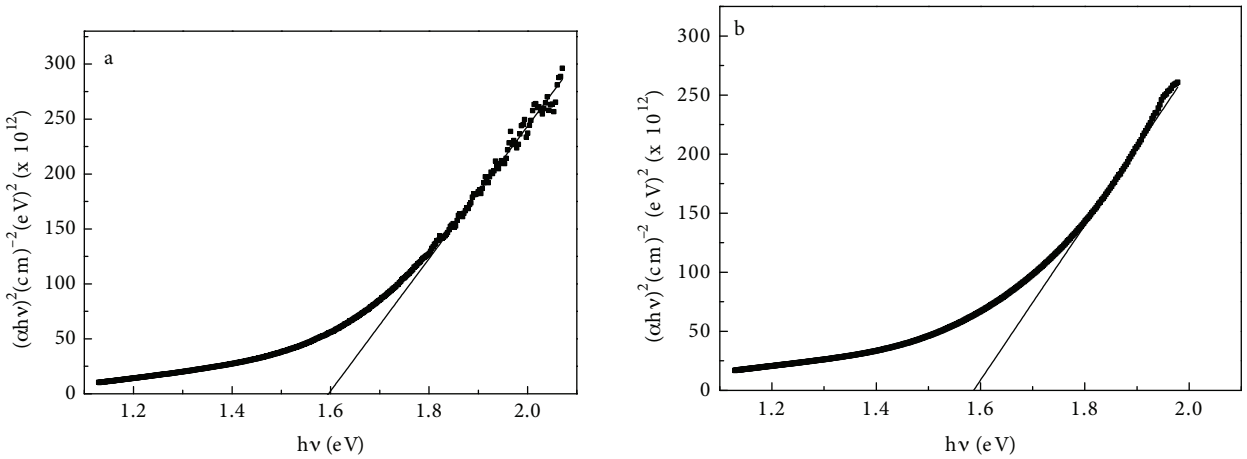

Figure 3. Optical absorption spectra of PbS films grown on **a)** glass substrate, **b)** GaSe crystal substrate.

The sheet charge carrier densities, sheet mobilities and sheet resistivities of PbS films grown on glass and GaSe substrates were measured between 120 and 290 K by the van der Pauw method. The results are given in Figures 4–6. As seen from these figures, PbS films grown on both substrates show p-type character

at low temperatures and n-type character at high temperatures. In the p-type region, the sheet charge carrier density was found to be 1.4 $\times$ 10^6–9 $\times$ 10^7 cm^{-2} for the PbS film grown on glass substrate, while it was 4.5 $\times$ 10^8–2 $\times$ 10^8 cm^{-2} for the PbS film grown on GaSe substrate (Figure 4). Similar behavior is observed in the temperature dependence of mobility. At this region the mobilities of PbS films grown on glass and GaSe substrates were found to be 35–278 cm^2/Vs and 92–154 cm^2/Vs, respectively (Figure 5). At the low temperature region, the conductivity of PbS films is due to the holes excited from the acceptor levels with ionization energies of 94.50 meV and 36.50 meV for the films grown on glass and GaSe substrates, respectively (Figure 6). In the n-type region, sheet charge carrier concentrations and mobilities were found to be 9.7 $\times$ 10^7–6.9 $\times$ 10^8 cm^{-2} and 2 $\times$ 10^8–5 $\times$ 10^8 cm^{-2} and 28–397 cm^2/Vs and 772–2487 cm^2/Vs for the PbS films grown on glass and GaSe substrates, respectively. The conductivity in this region is due to excitation of electrons from the donor centers with ionization energies of 226.50 meV and 310 meV for films grown on glass and GaSe substrates, respectively (Figure 6). In general, it is seen that the sheet charge carrier concentration and mobility of PbS film grown on GaSe substrate are higher than those grown on glass substrate.

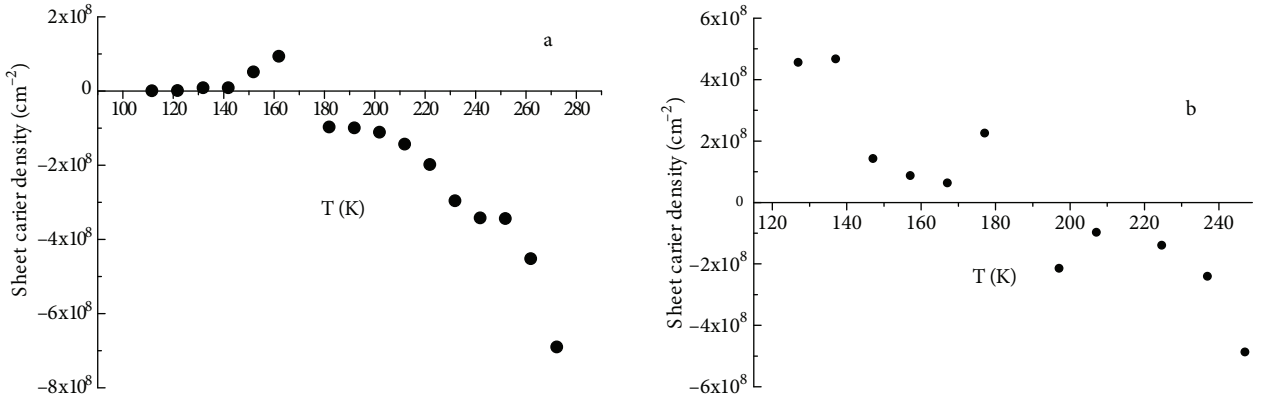

Figure 4. Temperature dependences of sheet carrier densities of PbS thin films grown on **a)** glass substrate, **b)** GaSe crystal substrate.

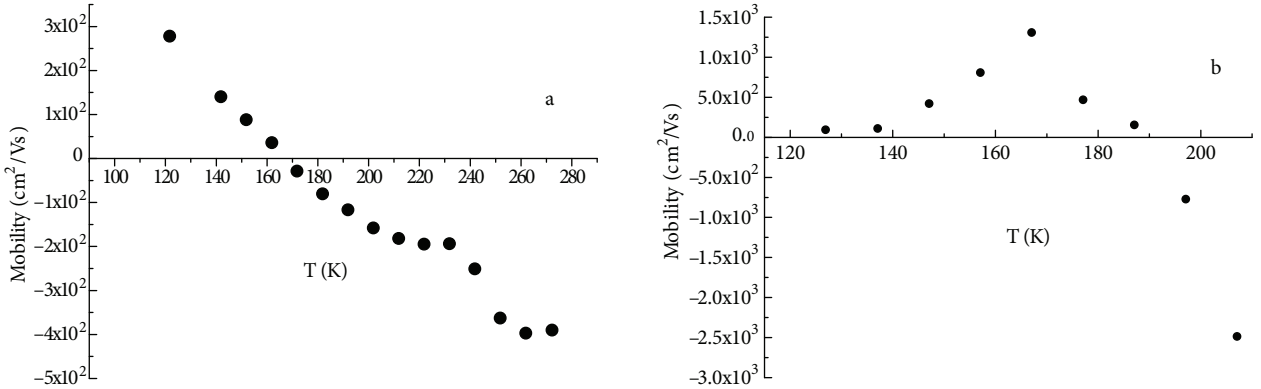

Figure 5. Temperature dependences of mobilities of PbS thin films grown on **a)** glass substrate, **b)** GaSe crystal substrate.

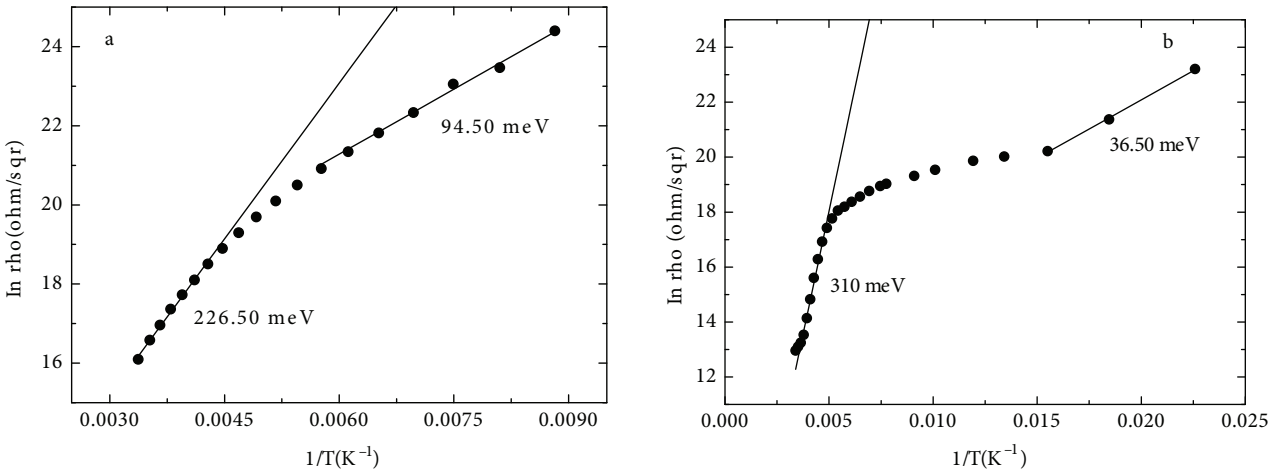

Figure 6. Temperature dependences of sheet resistivities of PbS thin films grown on **a)** glass substrate, **b)** GaSe crystal substrate.

4. Conclusions

The structure, surface morphology, optical absorption, and electrical properties of PbS films grown on glass substrate and on GaSe crystalline substrate by CBD were studied. The crystal structure of PbS films grown on both substrates is fcc, indicating that quasi van der Waals heterojunctions were formed at the GaSe–PbS interface. The band gap energies of PbS films grown on glass and GaSe substrates were found to be 1.60 eV and 1.59 eV, respectively. PbS films showed p- and n-type characters, depending on the temperature. At low temperatures, the p-type conductivity was determined by the acceptor centers while at high temperatures it was determined by the donor centers. In general, the sheet charge carrier concentration and mobility of PbS film grown on GaSe substrate were higher than those grown on glass substrate. The long wavelength tails of absorption spectra of PbS thin films grown on both glass and GaSe crystalline substrates showed exponential dependence with photon energy.

References

[1] Bube, R. H. *Photoelectronic Properties of Semiconductors*, Cambridge University Press: Cambridge, UK, 1992.

[2] Yang, P.; Song, C. F.; Lü, M. K.; Yin, X.; Zhou, G. J.; Xu, D.; Yuan, D. R. *Chem. Phys. Lett.* **2001**, *345*, 429–434.

[3] Hirata, H.; Higashiyama, K. *Bull. Chem. Soc. of Japan* **1971**, *44*, 2420–2423.

[4] Nair, P. K.; Nair, M. T. S. *J. Phys. D: Appl. Phys.* **1990**, *23*, 150–155.

[5] Sun, L.; Choi, J. J.; Stachnik, D.; Bartnik, A. C.; Hyun, B. -R.; Malliaras, G. G.; Hanrath, T.; Wise, F. W. *Nature Nanotechnology* **2012**, *7*, 369–373.

[6] Popescu, V. *Chemistry Magazine* (*Revista de Chimie*) **2004**, *2004/55*, 797–799.

[7] Popescu, V. *Chemistry Magazine (Revista de Chimie)* **2004**, *2004/55*, 983–985.

[8] Kane, R. S.; Cohen, R. E.; Silbey, R. *J. Phys. Chem.* **1996**, *100*, 7928–7932.

[9] Li, D.; Liang, C.; Liu, Y.; Qian, S. *J. Lumin.* **2007**, *122–123*, 549–551.

[10] Joshi, R. K.; Kanjilal, A.; Seghal, H. K. *Appl. Sur. Sci.* **2004**, *221*, 43–47.

[11] Seghaier, S.; Kamoun, N.; Brini, R.; Amara, A. B. *Mater. Chem. Phys.* **2006**, *97*, 71–80.

[12] Valenzuela-Jauregui, J. J.; Ramirez-Bon, R.; Mendoza-Galvan, A.; Sotelo-Lerma, M. *Thin Solid Films* **2003**, *441*, 104–110.

[13] Garcia-Valenzuela, J. A.; Baez-Gaxiola, M. R.; Sotelo-Lerma, M. *Thin Solid Films* **2013**, *534*, 126–131.

[14] Chaudhuri, T.; Saha, N.; Saha, P. *Mater. Lett.* **2005**, *59*, 2191–2193.

[15] Wang, S.; Pan, A.; Yin, H.; He, Y.; Lei, Y.; Xu, Z.; Zou, B. *Mater. Lett.* **2006**, *60*, 1242–1246.

[16] Ni, Y.; Wei, X.; Hong, J.; Ma, X. *Mater. Res. Bull.* **2007**, *42*, 17–26.

[17] Ni, Y.; Wei, X.; Hong, J.; Ma, X. *Cryst. Res. Technol.* **2006**, *41*, 885–888.

[18] Resch. R.; Friedbacher, G.; Grasserbauer, M.; Kanniainen, T.; Lindroos, S.; Leskela, M.; Niinistö, L. *Appl. Surface Sci.* **1997**, *120*, 51–57.

[19] Kanniainen, T.; Lindroos, S.; Resch, R.; Leskela, M.; Friedbacher, G.; Grasserbauer, M. *Mater. Res. Bull.* **2000**, *35*, 1045–1051.

[20] Puiso, J.; Tamulevicius, S.; Laukaitis, G.; Lindroos, S.; Leskela, M.; Snitka, V. *Thin Solid Films* **2002**, *403–404*, 457–461.

[21] Puiso, J.; Lindroos, S.; Tamulevicius, S.; Leskela, M.; Snitka, V. *Thin Solid Films,* **2003**, *428*, 223–226.

[22] Dong, L.; Chu, Y.; Liu, Y.; Li, M.; Yang, F.; Li, L. *J. Colloid Interface Sci.* **2006**, *301*, 503–510.

[23] Xu, L.; Zhang, W.; Ding, Y.; Yu, W.; Xing, J.; Li, F.; Qian, Y. *J. Cryst. Growth* **2004**, *273*, 213–219.

[24] Vossmeyer, T.; Katsikas, L.; Giersig, M.; Popovic, I. G.; Diesner, K.; Chemseddine, A.; Eychmüller, A.; Weller, H. *J. Phys. Cem.* **1994**, *98*, 7665–7673.

[25] Thangavel, S.; Ganesan, S.; Chandramohan, S.; Sudhagar, P.; Kang, Y. S.; Hong, C. H. *J. Alloy Com.* **2010**, *495*, 234–237.

[26] de la Rosa-Fox, N.; Erce-Montilla, R.; Pinero, M.; Esquivias, L. *Opt. Mater.* **2003**, *22*, 1–6.

[27] Koma, A. *Thin Solid Films* **1992**, *216*, 72–76.

[28] Koma, A. *J. Cryst. Growth* **1999**, *201/202*, 236–241.

[29] Lang, O.; Klein, A.; Pettenkofer, C.; Jaegermann, W.; Chery, A. *J. Appl. Phys.* **1996**, *80*, 3817–3821.

[30] Yang, S.; Wang, H.; Fu, W.; Kelley, D. F. *J. Photochemistry and Photobiology A: Chemistry* **2007**, *192*, 159–165.

[31] Mamedov, G. M.; Karabulut, M.; Kodolbaş, O.; Öktü, Ö. *Phys. Stat. Sol. B* **2005**, *242*, 2885–2891.

[32] Karabulut, M.; Bilir, G.; Mamedov, G. M.; Seyhan, A.; Turan, R. *J. Lumin.* **2008**, *128*, 1551–1555.

[33] Yang, Y. J.; Hu, S. *Thin Solid Films* **2008**, *516*, 6048–6051.

[34] Mammadov, G. M.; Karabulut, M.; Ertap, H.; Uğurlu, G.; Öztürk, M. K. *Azerbaijan J. Phys.* **2010**, *16*, 166–169.

[35] Guskov, A.; Camassel, J.; Guskov, L. *Prog. Cryst. Growth and Charact.* **1982**, *5*, 323–413.

[36] Osherov, A.; Ezersky, V.; Golan, Y. *Eur. Phys. J. Appl. Phys.* **2007**, *37*, 39–47.

[37] Pejova, B. *Mater. Res. Bull.* **2008**, *43*, 2887–2903.

[38] Pejova, B. *Mater. Chem. Phys.* **2010**, *119*, 367–376.